

The Magellanic Stream in Modified Newtonian Dynamics

Hossein Haghi ¹, Sohrab Rahvar ^{1,2}, Akram Hasani-Zonooz ³

haghi@mehr.sharif.edu

rahvar@sharif.edu

ABSTRACT

The dynamics of the Magellanic Stream (MS) as a series of clouds extending from the Magellanic Clouds (MCs) to the south Galactic pole is affected by the distribution and the amount of matter in the Milky Way. We calculate the gravitational effect of the Galactic disk on the MS in the framework of modified Newtonian dynamics (MOND) and compare with observations of the Stream's radial velocity. We consider the tidal force of the Galaxy, which strips material from the MCs to form the MS, and, using a no-halo model of the Galaxy, we ignore the effect of the drag of the Galactic halo on the MS. We also compare the MONDian dynamics with that in logarithmic and power-law dark halo models and show that the MOND theory seems plausible for describing the dynamics of satellite galaxies such as the MCs. Finally, we perform a maximum likelihood analysis to obtain the best MOND parameters for the Galactic disk.

Subject headings: dark matter – Galaxy: halo – gravitation – Magellanic stream – MOND.

1. Introduction

It has long been known that Newtonian gravity is unable to describe the dynamics of galaxies and clusters of galaxies correctly and that there is a discrepancy between the visible and the dynamical masses of galaxies. Nowadays, most astronomers believe that the universe is dominated by dark matter and that we can observe the gravitational effects of this matter in large-scale structure. Many observations have been dedicated to measuring the amount and nature of the dark matter. Gravitational microlensing is one of these experiments, designed to indirectly detect the dark matter of the halo in the form of MACHOs¹ (Alcock et al. 2000; Paczyński 1986). After almost two decades of microlensing experiments, it seems that MACHOs contribute a small fraction of the halo mass and that the microlensing events

toward the Large and Small Magellanic Clouds are most probably due to self-lensing by the Clouds (Sahu 2003; Tisserand & Milsztajn 2004; Rahvar 2004).

Other observations, such as of the abundances of the light elements from nucleosynthesis in the early universe and recent data from the *Wilkinson Microwave Anisotropy Probe* (*WMAP*) data, also rule out baryons as the dark matter. The best-fit baryon abundance, based on *WMAP* data, to a Λ CDM model is $\Omega_b h^2 = 0.0237^{+0.0013}_{-0.0012}$, implying a baryon-to-photon ratio of $\eta = 6.5^{+0.4}_{-0.3} \times 10^{-5}$ (Spergel et al. 2003). For this abundance, standard big bang nucleosynthesis (Burles et al. 2001) implies a primordial deuterium abundance relative to hydrogen of $[D/H] = 2.37^{+0.19}_{-0.21} \times 10^{-5}$, which is in the same range as observed in Ly α clouds (Kirkman et al. 2003): analysis of QSO HS 1243+3047 yields a D/H ratio of $2.42^{+0.35}_{-0.25} \times 10^{-5}$. WIMPs², as the other candidate for the so-called the cold dark matter (CDM), are motivated from non-standard particle physics. The problem with WIMPs is their small cross section

¹Department of Physics, Sharif University of Technology, P.O.Box 11365–9161, Tehran, Iran

²Institute for Studies in Theoretical Physics and Mathematics, P.O.Box 19395–5531, Tehran, Iran

³Department of Physics, Azarbaijan University of Tarbiat Moallem, Azarshahr, Tabriz, Iran

¹Massive compact halo object

²Weakly interactive massive particles

with ordinary matter, which would makes them difficult to observe, to date, no significant signal from experiments aimed at detecting such particles has been reported (Pretzl 2002; Green 2004; Goodman & Witten 1985; Jungman et al. 1996; Mirabolfathi 2005).

Another growing approach to explain the missing matter in the universe is a possible alternative theory of gravity. In these models, modification of the gravity law compensates for the lack of matter. One of the most famous alternative theories is modified newtonian dynamics (MOND), which was been introduced by Milgrom (1983). According to this phenomenological theory, the flat rotation curves of spiral galaxies at large radial distances can be explained with a modification of Newton's second law for accelerations below a characteristic scale of $a_0 \simeq 1 \times 10^{-8} \text{cms}^{-2}$ (Milgrom 1983; Bekenstein and Milgrom 1984; Sanders & McGaugh 2002). This theory, in addition to the acceleration parameter, a_0 , employs an interpolating function to connect and MONDian regimes. It has been shown that this simple idea may explain the dynamical motion of galaxies without resorting to dark matter (Pointecouteau & Silk 2005; Baumgardt et al. 2005; Scarpa et al. 2004). The parameters of this model can be fixed by various observations, such as the rotation curves of spiral galaxies. Recently, Famaey & Binney (2005) studied MOND in the context of the rotation curves of spiral galaxies, using different choices for the MOND interpolating function. Bekenstein (2004) presented a relativistic version of MOND, considering a Lorentz-covariant theory of gravity. Zhao & Famaey (2006) also examined different interpolating functions by fitting to a benchmark rotation curve, and they proposed a new set of interpolating functions that satisfy both weak and strong gravity. One of the main tests of MOND is its ability to produce power spectra that are compatible with the structures that we observe. Sanders (2001) showed that perturbations on small comoving scales enter the MOND regime earlier than those on larger scales and, therefore, evolve to large overdensities sooner. Taking the initial power spectrum from the cosmic microwave background, Sanders found that the evolved power spectrum resembled that of the standard CDM universe. However, studies by Nusser & Pointecouteau (2006) show that for a

spherically symmetric perturbation, in the framework of MOND, the gas temperature and density profiles evolve to a universal form that is independent of both the slope and amplitude of the initial density profile. While the obtained density profile is compatible with results from *XMM-Newton* and *Chandra* observations of clusters, the temperature profiles do not reconcile with the MOND prediction.

Another approach to examining MOND could be through the dynamics of the satellite galaxies around the Milky Way (MW). Read & Moore (2005) compared the precession of the orbit of the Sagittarius dwarf in a thin axisymmetric disk potential under MOND with that resulting from a thin disk plus nearly-spherical dark halo. They find that improved data on the leading arm of the Sagittarius dwarf, which samples the Galactic potential at large radii, could rule out MOND if the precession of the orbital pole can be determined to accuracy of a degree. Here we extend this work, using the dynamics of the Magellanic Stream (MS) to test MOND. The MS is a narrow band of neutral hydrogen clouds that extends along a curved path, starting from the Magellanic Clouds and oriented toward the south Galactic pole (van Kuilenburg 1972; Wannier & Wrixon 1972; Mathewson et al. 1974). We use the MONDian gravitational effect of a thin Kuzmin disk to represent the luminous part of the MW, and we obtain the dynamics of the MS, treating it as a quasi-steady flow. Using a maximum likelihood analysis, we find the best model parameters from an analysis of the MS radial velocity data reported by the Parkes Observatory (Brüns et al. 2005).

The paper is organized as follows: In §2, we give a brief review of the dark halo models for the Galaxy and of MOND theory as an alternative to dark matter. In §3, we introduce the Magellanic Stream and the main theories describing the distribution of gas along it. In §4, we compare the observed dynamics of the MS with predictions from CDM models and MOND theory, considering the MS as a quasi-steady flow. We conclude in §5.

2. Dynamics of The Milky Way: MOND Versus CDM

As pointed out in the previous section, there are two approaches for dealing with the problem of the

rotation curves of spiral galaxies. The first is to consider a dark halo around the galaxy that is 10 times more massive than its luminous component, and the second is to invoke an alternative theory such as MOND. In the first part of this section, we introduce MOND theory and consider a Kuzmin disk for the mass distribution of the Galaxy, and in the second part various dark matter models for the halo mass distribution in the MW are presented.

2.1. MOND

As mentioned in §1, the shortage of luminous matter in spiral galaxies and large-scale structures has motivated some astrophysicists to apply alternative theories. One possible approach to solve the dark matter problem is a change in Newtonian dynamics at small accelerations, so-called modified Newtonian dynamics (Milgrom 1983). In this model, Newton's second law is altered to read

$$\mu\left(\frac{|a|}{a_0}\right)\mathbf{a} = -\nabla\Phi_N, \quad (1)$$

where Φ_N is the Newtonian gravitational potential, \mathbf{a} is the acceleration, a_0 is an acceleration scale below which the dynamics deviates from the standard Newtonian form, and $\mu(x)$ is an interpolating function that runs smoothly from $\mu(x) = x$ at $x \ll 1$ to $\mu(x) = 1$ at $x \gg 1$ (i.e., the latter condition recovers Newtonian dynamics at accelerations that are large compared with a_0). Any successful underlying theory for MOND must predict an interpolating function. The functional form of $\mu(x)$ and the value of free parameters such as a_0 are usually chosen phenomenologically. The standard interpolating function used to fit with observations was introduced by Bekenstein & Milgrom (1984):

$$\mu(x) = \frac{x}{\sqrt{1+x^2}}. \quad (2)$$

Other functions have been suggested for $\mu(x)$, such as those of (Famaey & Binney 2005; Bekenstein 2004; Zhao et al. 2006). The typical value for the parameter a_0 , obtained from analysis of a sample of spiral galaxies with high-quality rotation curves is $a_0 = 1.2 \pm 0.27 \times 10^{-8} \text{ cm s}^{-2}$ (Begeman et al. 1991). Taking the divergence of both sides of equation (1) and substituting Poisson's equation in the right-hand side of equation (1) yields

$$\nabla \cdot \left(\mu\left(\frac{a}{a_0}\right)\mathbf{a}\right) = -4\pi G\rho. \quad (3)$$

For a given distribution of matter on the right-hand side of equation (3), the dynamics of the structure, depending on the interpolating function, can be found as

$$\mu\left(\frac{a}{a_0}\right)\mathbf{a} = G \int \mathbf{G}(\mathbf{x} - \mathbf{x}')\rho(x')dx'^3 + \nabla \times \mathbf{h}(\mathbf{x}) \quad (4)$$

where $\mathbf{G}(\mathbf{x})$ is the Green's function, G is the gravitational constant, and $\mathbf{h}(\mathbf{x})$ is an arbitrary vector field. Using the Green's function, equation (4) can be written in the form

$$\mu\left(\frac{|a|}{a_0}\right)\mathbf{a} = \mathbf{g}_N + \nabla \times h \quad (5)$$

where the first term on the right-hand side corresponds to the Newtonian gravitational acceleration and results from the distribution of the matter density. Since, with respect to the right-hand side of equation (5), $\nabla \cdot (\nabla \times h) = 0$, we can conclude from Gauss's theorem that on a boundary at infinity, $\nabla \times h$ falls faster than $1/r^2$, in other words, it can be ignored in comparison with the Newtonian acceleration (Bekenstein and Milgrom 1984). For the interpolating function $\mu(x)$ given in equation (2), we can obtain \mathbf{a} in terms of \mathbf{g}_N as follows:

$$\mathbf{a} = \mathbf{g}_N \left[\frac{1}{2} + \frac{1}{2} \sqrt{1 + \left(\frac{2a_0}{a_N}\right)^2} \right]^{1/2}. \quad (6)$$

Here we model the Galactic disk as a simple, infinitesimally thin Kuzmin disk (Kuzmin 1956), for which the corresponding Newtonian potential (Binney & Tremaine 1987) is given by

$$\phi_N(R, z) = \frac{-GM}{\sqrt{R^2 + (a + |z|)^2}}, \quad (7)$$

where a is the disk length scale and M is the mass of the disk. The question can be asked whether we can express the acceleration in the MOND regime in terms of the gradient of a scalar potential. To answer this question, we write the MONDian acceleration in terms of the Newtonian potential from equation (5) as follows:

$$\mathbf{a} = \nabla\varphi_N f(|\nabla\varphi_N|). \quad (8)$$

The acceleration is compatible with a scalar potential if the curl of the right-hand side of equation (8) vanishes. The condition $\nabla \times [\nabla\varphi_N f(|\nabla\varphi_N|)] = 0$ implies that $\nabla f(|\nabla\varphi_N|) \times \nabla\varphi_N = 0$, so in the case

of a Kuzmin disk, for which $|\nabla\varphi_N| = \varphi_N^2/GM$, we have $\nabla f(|\nabla\varphi_N|) \propto \nabla\varphi_N$, which means that $\nabla \times \mathbf{a} = 0$. A technique for constructing more general density-potential pairs in MOND has been introduced recently by Ciotti et al. (2006).

2.2. CDM Halo Models

In this subsection, we review the various halo models for the dark matter structure of Galaxy. Generic classes of these models are axisymmetric "power-law" and "logarithmic" models for the dark halo of the MW (Evans 1993, 1994). The gravitational potentials of the power-law and logarithmic models are given by

$$\Phi_G = \frac{V_a^2 R_c^\beta}{\beta(R_c^2 + R^2 + z^2 q^{-2})^{\beta/2}} \quad (9)$$

and

$$\Phi_G = -\frac{1}{2} V_a^2 \log(R_c^2 + R^2 + z^2 q^{-2}) \quad (10)$$

respectively. Poisson's equation gives the density distribution of the halo in cylindrical coordinates as

$$\rho(R, z) = \frac{V_a^2 R_c^\beta}{4\pi G q^2} \times \frac{R_c^2(1 + 2q^2) + R^2(1 - \beta q^2) + z^2[2 - (1 + \beta)/q^2]}{(R_c^2 + R^2 + z^2/q^2)^{(\beta+4)/2}}, \quad (11)$$

where the case $\beta = 0$ corresponds to a logarithmic model R_c is the core radius, and q is the flattening parameter (i.e., the axial ratio of the concentric equipotential). The parameter β determines whether the rotation curve asymptotically rises ($\beta < 0$), asymptotically falls ($\beta > 0$), or is flat ($\beta = 0$). At asymptotically large distances from the center of the Galaxy in the equatorial plane, the rotation velocity is given by $V_{circ} \sim R^{-\beta}$. The parameters of our halo models are given in Table 1.

For the Galactic disk, we use for the density of the disk the double exponential function

$$\rho(R, z) = \frac{\Sigma_0}{2h} \exp\left[-\frac{R - R_0}{R_d}\right] \exp\left[-\frac{|z|}{h}\right] \quad (12)$$

(Binney & Tremaine 1987), where z and R are cylindrical coordinates, R_0 is the distance of the Sun from the center of the MW, R_d is the length

scale, h is the scale height, and Σ_0 is the column density of the disk. The parameters of the disk models are also indicated in Table 1. The Galactic bulge is considered to be a point-like structure with mass $(1 - 3) \times 10^{10} M_\odot$ (Zhao & Mao 1996).

3. The Magellanic Stream

The *MS* is a narrow band of neutral hydrogen clouds with a width of about 8° that extend along a curved path, starting from the Magellanic Clouds (MCs) and oriented toward the south Galactic pole (Van Kuilenburg 1972; Wannier & Wrixon 1972; Mathewson et al. 1974). This structure comprises six discrete clouds, labeled MS *I* to MS *VI*, lying along a great circle from $(l = 91^\circ, b = -40^\circ)$ to $(l = 299^\circ, b = -70^\circ)$. The radial velocity and column density of this structure have been measured by many observational groups. Observations show that the radial velocity of the MS with respect to the Galactic center changes monotonically from 0 km s^{-1} at MS *I* to -200 km s^{-1} at MS *VI*, where MS *I* is located nearest to the center of the MCs and the MW, with a distance of ~ 48 kpc, and MS *VI* is at the farthest distance. Another feature of the MS is that the mean column density falls from MS *I* to MS *IV* (Mathewson et al. 1977; Mathewson et al. 1987; Brüns et al. 2005).

The MS is supposed to be an outcome of the interaction between the MCs and the MW, where the gravitational force of the MW governs the dynamics of the MS (Mathewson et al. 1987; Westerlund 1990; Fujimoto & Murai 1984; Wayte 1989). There are several models for the origin and existence of the MS, such as tidal stripping (Lin & Lynden-Bell 1982; Gardiner & Noguchi 1996; Weinberg 2000), ram pressure (Moore 1994; Sofue 1994) and continued ram pressure stripping (Liu 1992). In the diffuse ram pressure model, there is a diffuse halo around the Galaxy that produces a drag on the gas between the MCs and causes weakly bound material to escape from the region to form a tail. The discrete ram pressure models are based on collision and mixing of the density enhancements of the halo with the gas between the MCs to form the MS, and in the scenario of continued ram pressure stripping (Liu 1992), the MS is in a state of quasi-steady flow (i.e., $\frac{\partial v}{\partial t} = 0$). In the tidal model, the condition for quasi-steady flow

Model :	<i>S</i>	<i>A</i>	<i>B</i>	<i>C</i>	<i>D</i>	<i>E</i>	<i>F</i>	<i>G</i>
Description	Medium disk	Medium disk	Large halo	Small halo	Elliptical halo	Maximal disk	Thick disk	Thick disk
β	–	0	-0.2	0.2	0	0	0	0
q	–	1	1	1	0.71	1	1	1
$v_a(kms^{-1})$	–	200	200	180	200	90	150	180
$R_c(kpc)$	5	5	5	5	5	20	25	20
$R_0(kpc)$	8.5	8.5	8.5	8.5	8.5	7	7.9	7.9
$\Sigma_0(M_\odot pc^{-2})$	50	50	50	50	50	80	40	40
$R_d(kpc)$	3.5	3.5	3.5	3.5	3.5	3.5	3	3
$z_d(kpc)$	0.3	0.3	0.3	0.3	0.3	0.3	1	1

Table 1: Parameters of the Galactic models. The first line indicates the description of the models; the second line, the slope of the rotation curve ($\beta = 0$ flat, $\beta < 0$ rising and $\beta > 0$ falling); the third line, the halo flattening ($q = 1$ represent spherical); the fourth line, (v_a), the normalization velocity; the fifth line, R_c , the halo core; the sixth line, the distance of the Sun from the center of the Galaxy; the seventh line, the local column density of the disk ($\Sigma_0 = 50$ for canonical disk, $\Sigma_0 = 80$ for a maximal thin disk and $\Sigma_0 = 40$ for a thick disk); the eighth line, the disk length scale; and the ninth line, the disk scale height.

may be fulfilled by means of the tidal force of the Galaxy, which strips the HI clouds from the MCs. The Stream material then follows the same orbit as the MCs, such that the local velocity of the MS remains constant.

Recently, Brüns et al. (2005) reported on high-resolution observations of the radial velocity and column density of the MS. In the next section, we use these MS data to compare with the expected dynamics from the MOND and CDM scenarios. Comparing with the observations will enable us to place constraints on the parameters of the model.

4. Dynamics of The Magellanic Clouds

In this section, we obtain the dynamics of the MCs in MONDian theory, considering for the structure of the Galaxy an infinitesimally thin Kuzmin disk without a dark halo component. In this model, since we have ignored the Galactic halo, there is no drag force from the halo on the MS, and the main factor in the stripping of the MS is the tidal force exerted by the Galactic disk. Using the gradient of the gravitational force imposed by the Galaxy on the MCs, we can make an estimate of the tidal radius, the distance from the MCs beyond which all the material can escape from the structure.

In the Newtonian case, we consider a structure with mass M_s rotating in an orbit around

the Galaxy, which has a halo of size R_G and mass M_G . The acceleration at the center of this structure is GM_G/R_G^2 , while the acceleration at a distance r from its center toward the Galaxy is $GM_G/(R_G - r)^2$, for $R_G \gg r$, the difference between these will be $g_G = 2GM_G r/R_G^3$. On the other hand, the acceleration imposed toward the structure is $g_s = GM_s/r^2$. So, material will move away in the direction of the Galaxy if $g_G > g_s$, which implies a stability radius of $r_{tidal} = R_G(2\frac{M_s}{M_G})^{1/3}$ (von Hoerner 1957). For the deep MOND regime, $\mu(x) \simeq x$ and the MONDian and Newtonian accelerations are related through $a \simeq (a_0 g_N)^{1/2}$. The tidal acceleration, similarly to the Newtonian case, obtains as the difference between the acceleration in the MCs and at a distance r from them as

$g_G = GM_G a_0^{1/2} r/R_G^2$. On the other hand, we have the gravitational acceleration toward the MCs at the distance r , which is $g_s = GM_s a_0^{1/2}/r$, and so for the tidal radius we obtain $r_{tidal} = R_G(\frac{M_s}{M_G})^{1/4}$. If we take the same mass-to-light ratio for the Galaxy as for the Clouds, we can say that the tidal radius in the MONDian regime is of the same order as that in the dark matter model. Let the ratio of the luminous matter of the MCs to that in the Galactic disk be of order 10^{-2} ; for $R_G \simeq 50kpc$, we obtain in the MONDian regime a tidal radius of about $\simeq 15kpc$, versus $\simeq 13kpc$ in the dark matter model.

<i>Model</i>	S	A	B	C	D	E	F	G	MOND	MOND (M. L.)
χ^2	526	816	2285	437	576	1511	562	315	810	356

Table 2: Minimum χ^2 from fitting with various Galactic models. The Cold Dark matter halo models are labeled with of *S*, *A*, ... *G* with the corresponding values for the parameters of the models, indicated in Table 1. The last column corresponds to the minimum χ^2 from the Maximum Likelihood analysis in the MOND model.

<i>Model</i>	$M(M_\odot)$	a	b	c	v_0	R_c	q	$M_b(M_\odot)$	$a_0(ms^{-2})$	χ^2
<i>MOND</i>	1.2×10^{11}	4.5	-	-	-	-	-	-	1.2×10^{-10}	356
<i>CDM</i>	1.2×10^{11}	4.5	-	-	175	13	1	-	-	343
<i>f095CDM</i>	1.2×10^{11}	4.5	-	-	175	13	0.95	-	-	349
<i>f09CDM</i>	1.2×10^{11}	4.5	-	-	175	13	0.9	-	-	361
<i>f1.25CDM</i>	1.2×10^{11}	4.5	-	-	175	13	1.25	-	-	341
<i>L05</i>	1×10^{11}	6.5	0.26	0.7	171	13	0.9	3.53×10^{10}	-	362

Table 3: Comparison of MS data with the MOND and CDM Galactic halo models. The first line is the usual MOND model, the second to the fifth lines correspond to the CDM models (Johnston et al. 2005 and Law et al. 2005) The parameters *a*, *b*, *c* and R_c are in *kpc* and v_0 is in terms of *km/s*. See Read and Ben Moore (2005) for more details of the models.

According to the quasi-steady flow model, the MS will lie in the same orbital path as the MCs, so the location and velocity of the MS can represent the dynamics of the MCs. Here we are looking to the radial velocity of the MS toward the Galactic center to compare with observations. As a result of hydrodynamic friction, the MCs could have their motion damped and fall toward the Galaxy in a spiral path. However, since in this model there is no halo around the Galaxy, we can ignore friction forces. Substituting the Newtonian potential of the Kuzmin disk (eq. [7]), the MONDian potential in cylindrical coordinates is obtained

$$\phi_M = \frac{\sqrt{GMa_0}}{2} \ln(R^2 + (a + |z|)^2), \quad (13)$$

as (Read & Moore 2005; Brada & Milgrom 1995). For convenience, we carry out a coordinate transformation from the cylindrical to the spherical frame and obtain the components of the acceleration as follows:

$$a_r = -\sqrt{MGa_0} \left(\frac{a \cos \theta + r}{2ar \cos \theta + r^2 + a^2} \right) \quad (14)$$

$$a_\theta = -\sqrt{MGa_0} \left(\frac{a \sin \theta}{2ar \cos \theta + r^2 + a^2} \right), \quad (15)$$

$$a_\phi = 0, \quad (16)$$

where a_ϕ is zero as a consequence of the cylin-

drically symmetric distribution of matter around the *z*-axis. To solve the equation of motion, we take the location and velocity of MS *I* as the initial conditions for the dynamics of the MCs. Since MS *I* is located closest to the center of Galaxy, it almost has only a transverse velocity component with respect to the Galactic center. Although, there are no indicators at MS *I* by which to measure its transverse velocity, we can nevertheless use the transverse velocity of the MCs measured from the kinematics of planetary nebulae in the LMC, $v_\theta = 281 \pm 41 km s^{-1}$ (van der Marel et al. 2002) as an estimate of the transverse velocity of MS *I*. We utilize the conservation of angular momentum for the dynamics of the MCs (i.e., $r_{MCs} v_{MCs} = r_{MSI} v_{MSI}$), which provides an MS *I* transverse velocity on the order of $v_\theta(r_0) = 320 \pm 50 km s^{-1}$. Here the distance of MS *I* has been taken to be $r_0 = 48 \pm 1 kpc$.

In what follows, we compare the dynamics of the MCs with observation. Figure 1 shows the observed radial velocity of the MS in terms of the angular separation of from the MCs in a frame centered on the Galaxy. Since we are interested in comparing the global motion of the MS with the model, the internal dynamics of the structure has been ignored. The radial velocity of the MS

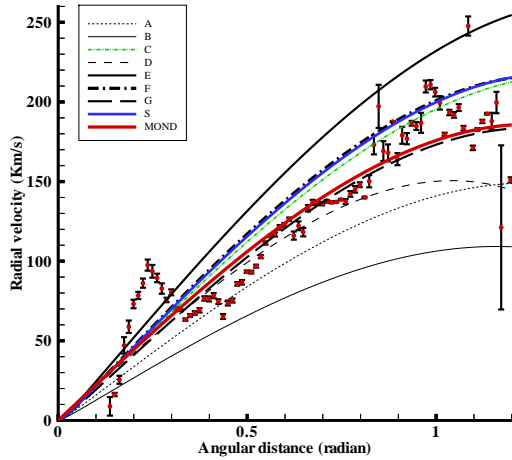


Fig. 1.— Radial velocity v_r vs. angular distance θ along the MS in the center of Galactocentric frame. The observational data (Brüns et al. 2005) are compared with theoretical curves obtained from MONDian and CDM models. The minimum χ^2 corresponding to each curve is given in Table 2. [See the electronic edition of the Journal for a color version of this figure.]

is calculated by averaging over the data at each point of the Stream and the error bars on the radial velocity result from the dispersion velocity of the structure. This velocity dispersion is caused by substructural motions of the MS such as the stochastic behavior of gas, and for different realizations of the MS, the dispersion velocity will be different at each point. The observed data are a continuum distribution of radial velocities in terms of angular separation; however, we collected data for each cluster of gas and obtained the average velocity and the corresponding dispersion velocity. We use χ^2 fitting,

$$\chi^2 = \sum_i^N \left(\frac{V_{th}^i - V_{obs}^i}{\sigma_i} \right)^2, \quad (17)$$

for comparison of the observed data and dynamics of the MS from the MOND and CDM models (see Fig. 1). We should take into account that the CDM and MOND models in these cases have different mass distributions.

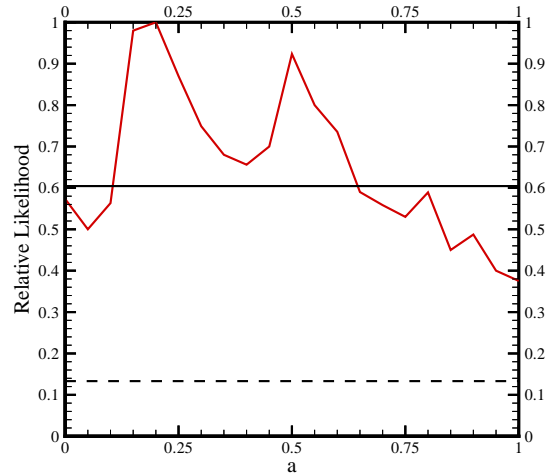
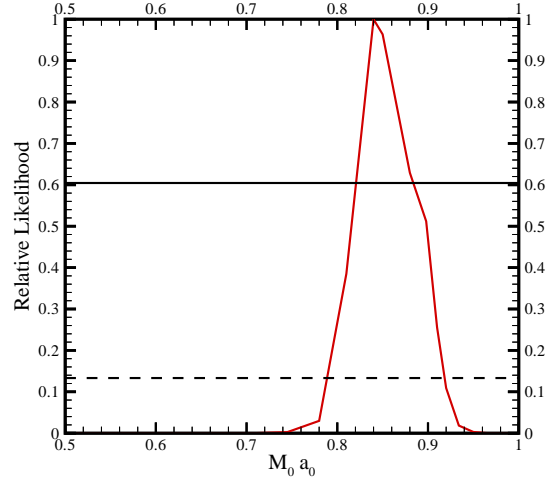


Fig. 2.— Marginalized likelihood functions of the parameters of the MOND and Kuzmin disk. Top, product of the disk mass M_0 ($10^{11}M_\odot$) and the MOND acceleration scale a_0 ($10^{-10}ms^{-2}$); bottom, length scale of the Kuzmin disk. The intersection of the curves with the horizontal solid and dashed lines give the bounds at 1σ and 2σ confidence levels, respectively. [See the electronic edition of the Journal for a color version of this figure.]

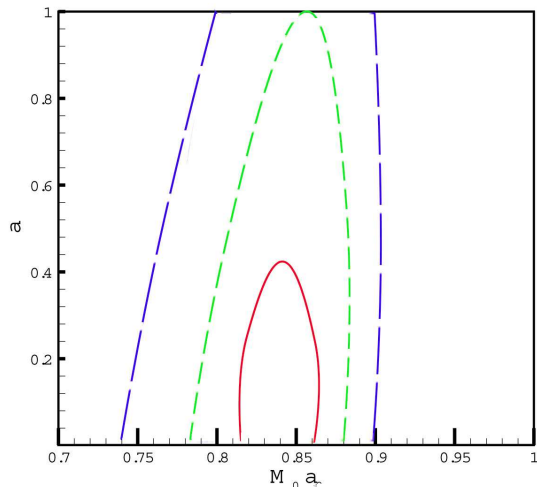


Fig. 3.— Joint confidence intervals for $M_0 a_0 (10^{11} M_\odot \times 10^{-10} \text{ms}^{-2})$ and the disk length scale $a (\text{kpc})$, with 1σ (solid line), 2σ (dashed line), and 3σ long-dashed line confidence levels. The minimum value of χ^2 corresponds to $a = 0.2_{-0.1}^{+0.45} \text{kpc}$ and $M_0 a_0 = 0.84_{-0.02}^{+0.05}$. [See the electronic edition of the Journal for a color version of this figure.]

The dark matter models are labeled *S*, *A*, *B*, *C*, *D*, *E*, *F*, and *G* with their corresponding parameters in Table 1. The minimum χ^2 values from fitting with the CDM and MOND models are listed in Table 2. We performed a maximum likelihood analysis to find the best parameters for MOND. Comparing the minimum value of χ^2 from the modified dynamics with those of the dark matter models shows that MOND results in a better fit than the CDM models, except for model *G*. The best parameters for a MONDian potential and the characteristic acceleration parameter, from the maximum likelihood analysis, are found to be $M_0 a_0 = 0.84_{-0.02}^{+0.05}$ and $a = 0.2_{-0.1}^{+0.45} \text{kpc}$, where M_0 is the mass of the disk in terms of $10^{11} M_\odot$, a_0 is the MOND acceleration scale in terms of 10^{-10}ms^{-2} and a is the length scale of the Kuzmin disk. The marginalized relative likelihood functions for $M_0 a_0$ and a are shown in Figure 2, Figure 3 shows the joint confidence intervals for $M_0 a_0$ and a with 1σ to 3σ confidence levels.

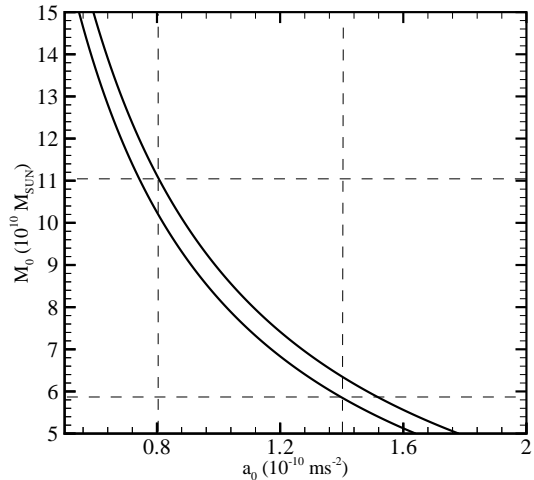


Fig. 4.— Constraints on $M_0 a_0 = 8.4_{-0.2}^{+0.5}$ from the maximum likelihood analysis, with 1σ confidence interval (M_0 in terms of $10^{10} M_\odot$ and MONDian acceleration scale a_0 in terms of 10^{-10}ms^{-2}). Using the range $a_0 = 0.8 - 1.4$ implies $M_0 = 6 - 11$ for the mass of the Kuzmin disk. [See the electronic edition of the Journal for a color version of this figure.]

As can be seen from the results of the maximum likelihood analysis, in MOND the length scale of the Kuzmin disk favor small values, in the range $a < 1 \text{kpc}$ with a wide error bar. We can interpret this as a consequence of the MS being located at a large distance from the Galaxy compared with a , which means that the dynamics of the MS is not sensitive to this length scale. $M_0 a_0$ is also confined to a range of about 0.8 to 0.9. In order to break the degeneracy between the mass of the disk and the acceleration scale of MOND (a_0), we use the luminous mass of the MW to constrain the parameter a_0 . The total luminosity of the Galactic disk is $1.2 \times 10^{10} L_\odot$ (Binney & Tremaine 1987), and if we assume an average stellar mass-to-light ratio of $\Upsilon = 5$, the total stellar mass of the Galactic disk should be about $M_* \simeq 6 \times 10^{10} M_\odot$; using the constraint $M_0 a_0 \simeq 0.84$ then results in $a_0 \simeq 1.4$. Comparing the value $a_0 = 1.2 \pm 0.27$ from analysis of the rotation curves of spiral galaxies (Begeman et al. 1991), with that from our analy-

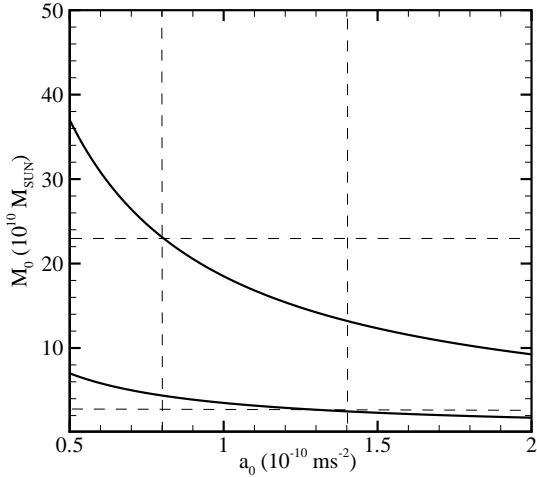


Fig. 5.— Constraints on $M_0 a_0$ considering 2σ error bars on the initial value for the transverse velocity of MS *I*. Using the preferred value $M_* \simeq 6 \times 10^{10} M_\odot$ for the Galactic disk yields $a_0 = 0.8 - 1.4$; alternatively, adopting a MOND acceleration scale in the range $a_0 = 0.8 - 1.4$ implies a disk mass in the range $M_0 = (2.5 - 23) \times 10^{10} M_\odot$. [See the electronic edition of the Journal for a color version of this figure.]

sis of the MS, we see good agreement. If, in addition to the contribution of the disk to the Galactic mass, we add the lower and upper limits for the mass of the Galactic bulge, the total mass of the Galaxy lies in the range $(4.3 - 12.8) \times 10^{10} M_\odot$ (Sackett 1997; Zhao et al. 1995), which confines the value of a_0 to $0.65 - 1.95$. In addition, for the range of the MOND acceleration scale adopted in the literature, $a_0 = 0.8 - 1.4$, the mass of the disk is found to be $M_0 = (6 - 11) \times 10^{10} M_\odot$ (see Fig. 4).

In the likelihood analysis here, we used as an initial condition the central value of the velocity of MS *I* without taking into account the corresponding error bar. In order to check the sensitivity of our results to the uncertainty in the velocity of the MCs, we repeated the likelihood analysis for an MS *I* transverse velocity in the range $v_{MSI} = 320 \pm 100$ with 2σ error bars. Figure 5 shows that $M_0 a_0$ is constrained to $M_0 a_0 =$

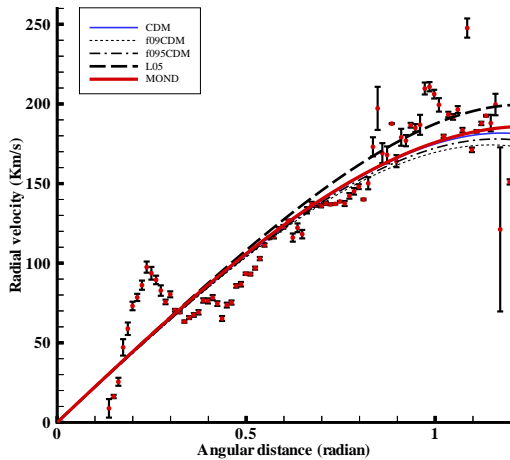


Fig. 6.— Same as Fig. 1, but for recent CDM models of the Galactic halo form studies of the tidal debris from the Sagittarius dwarf galaxy (see Table 3). [See the electronic edition of the Journal for a color version of this figure.]

$0.84^{+1.01}_{-0.53}$ when considering this uncertainty on the initial value for MS *I*'s transverse velocity. Using the preferred value of $M_* \simeq 6 \times 10^{10} M_\odot$ for the Galactic disk confines the acceleration scale to the range $a_0 = 0.8 - 1.4$. Alternatively, considering the literature acceleration scale for MOND of $a_0 = 0.8 - 1.4$ provides a Galactic disk mass of $M_0 = 2.5 - 23 \times 10^{10} M_\odot$, a larger range than that of our previous analysis. For the standard value of $a_0 = 1.2$, the mass of the Galactic disk is confined to $M_0 = 3 - 15 \times 10^{10} M_\odot$. Higher accuracy observations of the transverse velocity of the MCs will provide a better constraint on the parameters of the model.

Finally, we compare the dynamics of the MS in MOND with recent CDM Galactic halo models proposed to interpret the dynamics of the Sagittarius dwarf galaxy around the MW (Read & Moore 2005). Figure 6 compares the observed radial velocity of the MS with these Galactic models, and Table 3 indicates the best-fit value of χ^2 for each model and shows that the MOND result is almost compatible with the CDM models.

5. Conclusion

In this work, we used recent observational data on the radial velocity of the Magellanic Stream to examine modified Newtonian dynamics. The MS is considered to be a trace of the Magellanic Clouds produced by the interaction of the Clouds with the Galaxy. We considered the MONDian tidal effect of the Galaxy as the origin of the MS. For simplification, in our analysis we used the quasi-steady model for the flow of the MS, considering this structure to follow the same orbit, with the same dynamics, as the MCs. The radial velocity of this structure was compared with the observations, allowing us to place constraints on the product of the Galactic disk mass and the MOND acceleration scale ($M_0 a_0$). The range for the mass of the Galaxy obtained from this analysis is compatible with the observed luminous mass of the disk. Comparing the best fit from MOND with cold dark matter models for the halo shows that MOND fits the observations as well as the conventional halo models (Read & Moore 2005; Helmi 2004; Johnston et al. 2005; Hasani-Zonooz et al. 2005).

We should point out that while the dynamics of the MS in this model is in good agreement with the observations, a problem with this tidal model could be the lack of corresponding stellar tidal debris in the MS ((Moore & Davis 1994; Guhathakurta & Reitzel 1998)). Despite our expectation in the tidal model that stars should have been stripped off with the gas, observations show that stellar tails are often completely missing or are offset from the gaseous tails in interacting systems (e.g., the M82 Group; Yun et al. 1994; Hibbard et al. 2000). In the case of a MONDian tidal model, since the tidal radius is larger than in the Newtonian case, we expect a Galactic structure with a gas distribution that is more extended than the stellar component form of the MS. So, we should be observing mainly the gaseous component in the MS. N-body simulations of tidal stripping of the MS from the MCs in the MONDian regime without a Galactic halo will give a better view of this model and enable us to compare the density distribution of the gas in the MS with observations.

The authors thank J. I. Read for studying the

manuscript and providing very useful comments, and M. Nouri-Zonoz, M. A. Jalali, and M. S. Movahed for improving the text. We would also like to thank an anonymous referee for very useful comments. S.R. thanks Alain Omont and the Institut d'astrophysique de Paris, where a part of this work was done, for their hospitality.

REFERENCES

- Alcock, C., et al. 2000, *ApJ*, 542, 281
- Baumgardt H., Grebel E.K. and Kroupa P. 2005, *MNRAS*, 359, L1
- Bekenstein J.D., Milgrom M., 1984, *ApJ*, 286, 7
- Bekenstein J., 2004, *PRD*, 70, 083509
- Begeman K.G., et al, 1991, *MNRAS*, 249, 523
- Binney S., Tremaine S., 1987, *Galactic Dynamics*, Princeton Univ. Press, Princeton, NJ
- Brada R., Milgrom M., 1995, *MNRAS*, 276, 453
- Brüns, C., et al. 2005, *A&A*, 432, 45
- Burles, S., Nollett, K. M., & Turner, M. S. 2001, *ApJ*, 552, L1
- Ciotti L., Londrillo P. and Nipoti C., 2006, *ApJ*, 640, 741.
- Evans N. W., 1993, *MNRAS*, 260, 191
- Evans N. W., 1994, *MNRAS*, 267, 333
- Famaey B., Binney J., 2005, *MNRAS*, 361 633
- Fujimoto M., Murai T., 1984, *Structure and Evolution of the Magellanic clouds*, IAU symp. No. 108, 115.
- Gardiner, L. T., Noguchi, M. 1996, *MNRAS*, 278, 191
- Goodman M., Witten E., 1985 , *Phys. Rev. D*31, 3059.
- Green A.M., 2003, to appear in the proceedings of IAU Symposium 220 "Dark matter in galaxies", ASP, Eds: S. Ryder, D.J. Pisano, M. Walker, K. Freeman, (astro-ph/0310215)

- Guhathakurta, P., Reitzel, D. B. 1998, in ASP Conf. Ser. 136, Galactic Halos: A UC Santa Cruz Workshop, ed. D. Zaritsky (San Francisco: ASP), 22
- Hasani-Zonooz A., Haghi H., Rahvar S., (astro-ph/0504171)
- Helmi A., 2004, ApJ, 610, L97
- Hibbard, J. E., Vacca, W. D., Yun, M. S. 2000, AJ, 119, 1130
- Johnston K.V., et al , 2005, ApJ, 619, 800
- Jungman G., et al, 1996, Phys. Rep. 267(no 5-6), 195
- Kuilenburg , J. V., 1972, A&A, 16, 276
- Kuzmin , G. G., 1956, AZh, 33, 27
- Kirkman, D., Tytler, D., Suzuki, N., OMeara, J., & Lubin, D., 2003, ApJS, 149, 1
- Lin D. N. C., Lynden-Bell D., 1982, MNRAS 198, 707.
- Liu Y., 1992, A&A 257, 505
- Mathewson D.S., Cleary M.N., Murray J.D., 1974, ApJ, 190, 291
- Mathewson D.S., Schwarz M.P., Murray J.D., 1977, ApJ, 217, L5
- Mathewson D.S., Wayte S.R., Ford V.L., Ruan K., 1987, Proc. Astron. Soc. Aust. 7, 19.
- Meatheringham S. J., et al, 1988, ApJ, 327, 651
- Milgrom M., 1983, ApJ, 270, 365
- Mirabolfathi N., Invited talk at the XXIV Physics in Collisions Conference (PIC04), Boston, USA, June 2004, (astro-ph/0412103)
- Moore B., 1994, Nature 370, 629.
- Moore B., Davis M., 1994, MNRAS 270, 209
- Nusser, A., Pointecouteau, E., 2006, MNRAS, 366, 969
- Paczyński B., 1986, ApJ, 304, 1
- Pointecouteau E., Silk P. , 2005, MNRAS, 364, 654-658, (astro-ph/0505017).
- Pretzl K., 2002, Space Science Reviews, v. 100, Issue 1/4, p. 209-220.
- Rahvar S., 2004, MNRAS, 347, 213.
- Read J.I , Ben Moore, 2005, MNRAS, 361 , 971-976.
- Sahu K, C., 2003, "To appear in the Proceedings of the STScI Symposium on "Dark Universe: Matter, Energy, and Gravity" (astro-ph/0302325).
- Sanders, R. H., 2001, ApJ, 560, 1
- Sanders R. H., McGaugh S., 2002, Ann. Rev. Astron. Astrophys., 40, 263.
- Sackett P.D., 1997, ApJ, 483, 103-110
- Scarpa R., Marconi G., Gilmozzi R., 2003, IAU220 symposium "Dark matter in galaxies", (astro-ph/0308416)
- Sofue, Y., 1994, PASJ, 46, 431
- Spergel, D. N., et al, 2003, APJS 148, 175
- Tisserand, P., Milsztajn, A., 2004, appear in the proceedings of the 5th Rencontres du Vietnam, "New Views on the Universe",
- van der Marel R.P., et al, 2002, AJ, 124, 2639-2663
- von Hoerner S., 1957, ApJ, 125, 451
- Wannier P., Wrixon G.T., 1972, ApJ, 173, L119
- Wayte S. R., 1989, Proc. Astron. Soc. Aust.8, 195
- Westerlund B. E., 1990, A&A R 2, 29
- Weinberg, M. D., 2000, ApJ, 532, 922
- Yun M. S., Ho P. T. P., Lo K. Y. 1994, Nature, 372, 530
- Zhao H., Mao S., 1996, MNRAS, 283, 1197Z.
- Zhao H., Spergel D.N., Rich R.M., 1995, ApJ,440L, 13Z
- Zhao H., Bacon D.J., Taylor A.N., Horne K., 2006, MNRAS, 368, 171 (astro-ph/0509590).
- Zhao H.S, Famaey B, 2006, ApJ,638, L9-L12 (astro-ph/0512425)

This 2-column preprint was prepared with the AAS L^AT_EX macros v5.2.